9

Mohd Dilshad Ansari*, Satya Prakash Ghrera and Arunodaya Raj Mishra

Texture Feature Extraction Using Intuitionistic Fuzzy Local Binary Pattern

DOI 10.1515/jisys-2016-0155

Received August 24, 2016; previously published online December 8, 2016.

Abstract: In this paper, intuitionistic fuzzy local binary for texture feature extraction (IFLBP) has been proposed to encode local texture from the input image. The proposed method extends the fuzzy local binary pattern approach by incorporating intuitionistic fuzzy sets in the representation of local patterns of texture in images. Intuitionistic fuzzy local binary pattern also contributes to more than one bin in the distribution of IFLBP values, which can further be used as a feature vector in the various fields of image processing. The performance of the proposed method has been demonstrated on various medical images and processing images of size 256×256 . The obtained results validated the effectiveness and usefulness of our proposed method over the other reported methods, and new improvements are suggested.

Keywords: Fuzzy local binary pattern, intuitionistic fuzzy sets, intuitionistic fuzzy local binary pattern, entropy.

1 Introduction

Feature extraction is a process to extract the compact and essential information from an image. The major objective of feature extraction is to find the most significant information from original or raw data. When the input image or data to an algorithm is excessively bulky to be processed, it is supposed to be redundant (a large amount of data but a little information). Afterwards, the input data will be transformed into a highly reduced dimension representation or a set of features (also known as features vector). These extracted feature vectors represent the whole image. If extracted features are carefully selected, it is expected that the feature set will extract significant information in order to carry out the preferred task using this reduced representation instead of input image or full data. Extracted features have been used in various fields of image processing and signal processing, such as image forensics, remote sensing, pattern recognition, visual inspection, object discrimination, biomedical image processing, character recognition, terrain delimitation, image classification, document verification, reading bank deposit slips, applications for credit cards, and script recognition [3, 4, 8, 10, 28, 45, 46, 48].

The most common features available in an image include color, texture, and shape. Feature extraction is mainly dependent on these three types of features, and the performance of any desired task is also dependent on these extracted features. Generally, feature representation methods are divided in three categories: global, block-based, and region-based features [10, 45]. Less concentration has been given to image feature extraction compared to a significant amount of research on the construction of annotation/retrieval model itself. Therefore, in this paper, our attention is only on texture-based feature extraction. We have tested our algorithm on various medical images, i.e. X-ray, thyroid and brain computed tomography (CT) scan, and image processing images, i.e. Lena image and JUIT logo.

^{*}Corresponding author: Mohd Dilshad Ansari, Department of Computer Science and Engineering, Jaypee University of Information Technology, Waknaghat, Solan, Himachal Pradesh, India, e-mail: m.dilshadcse@gmail.com

Satya Prakash Ghrera: Department of Computer Science and Engineering, Jaypee University of Information Technology, Waknaghat, Solan, Himachal Pradesh, India

Arunodaya Raj Mishra: Department of Mathematics, ITM University, Gwalior, Madhya Pradesh, India

A number of textural feature extraction methods have been proposed [36, 47]. The local binary pattern (LBP) method [34], which is based on the concept of binary patterns (BPs) for representation of texture, has been broadly adopted because it is simple yet effective in describing the local spatial structure of an image. The LBP approach has been extended and combined with other approaches, resulting in a wide range of texture representation schemes suitable for different image analysis tasks. Typical examples include LBP extensions featuring scale invariance [9], rotation invariance [12, 38], combination of inter- and intra-spatial structure of the LBP patterns [49], and fusion of micro-LBP and macro-Gabor features [30].

2 Related Work

One of the first studies on visual inspection [22] has shown that LBP features can be successfully used for surface defect detection. Later, in Ref. [42], BP-based features have been used for wood quality discrimination, and more recently such features have also been applied on automatic defect detection [16, 44] as well as in remote sensing [14]. A variety of studies have shown that the BP-based feature extraction approaches are suitable for content-based image retrieval [23, 29], whereas recently the LBP approach has been adopted in a discriminative model for image ranking from text queries [15]. Moreover, in the area of face recognition, the LBP is recognized as a highly efficient texture representation approach. For example, it has been used for invariant face recognition [43, 52], face authentication [11], and the recognition of facial expressions [40]. Excellent results have also been obtained from its application on biomedical domain, including video endoscopy [20], the classification of protein images [33], and computer-aided neuroblastoma prognosis system [39]. In the area of motion analysis, the application of BP-based approaches has been investigated for underwater image matching [13], modeling and detection of moving objects [19], and object tracking [37].

The research community has a lot of interest on LBP texture representation, and various approaches have been proposed based on the BP model. An approach has been proposed for the estimation of a local contrast measure [34]. The LBP/C approach, which is based on the joint distribution of LBP codes and local contrast measures, has shown resistance to variations of the illumination. It has been used to enhance the discrimination ability of the original LBP approach [34]. Another variation of LBP is the local edge patterns approach, which has been proposed for image segmentation [50]. It describes the spatial structure of local texture according to the spatial arrangement of edge pixels. In the same spirit, Hafiane et al. [17] proposed median BP (MBP), which is intensity-shift invariant. According to this approach, the texture primitives are determined by localized thresholding against the local median. In a subsequent study, a hashed version of MBP to a binary chain or equivalence class has been evaluated, resulting in a resolution- and rotation-invariant MBP texture descriptor [18].

Fuzzy sets provide a flexible framework for handling the indeterminacy characterizing real-world systems, arising mainly from the imprecise and/or imperfect nature of information. However, fuzzy sets do not cope with the hesitancy (intuitionistic index) in images that originate from various factors, which in their majority are caused by inherent weaknesses of the acquisition and imaging mechanisms. Distortions that occur as a result of the limitations of acquisition chain, such as quantization noise, the suppression of dynamic range, or the non-linear behavior of the mapping system, affect our certainty regarding the "brightness" or "edginess" of a pixel, and therefore introduce a degree of hesitancy associated with the corresponding pixel. The fuzzy sets theory was introduced by Zadeh [51] on the extraction of texture spectrum features [7] and their efficient successors. The LBP features could possibly enhance their robustness to noise [21, 24–27]. However, these studies can only be considered as preliminary as they include only a limited experimental evaluation. Iakovidis et al. [21] and Keramidas et al. [27] proposed a generic, uncertainty-aware methodology for the derivation of fuzzy LBP (FLBP) texture models. Additionally, the intuitionistic fuzzy set theory proposed by Atanassov [5] and Atanassov and Gargov [6] provides a flexible mathematical framework to cope with uncertainty with the hesitancy originating from imperfect or imprecise information [31, 32]. A prominent characteristic of IFS is that it assigns to each element a membership degree and a non-membership degree with a certain amount of hesitation degree. In this paper, we propose intuitionistic FLBP (IFLBP) for texture representation using Atanassov's intuitionistic fuzzy sets.

2.1 Local Binary Pattern

LBP is a kind of gray-scale texture operator that is used for describing the spatial structure of an image texture [34]. The LBP texture model is based on the comparison of pixel values of a pixel neighborhood. A binary value is assigned to each pixel p_{\cdot} , belonging to a local neighborhood. This value is calculated by comparing the value of a pixel intensity g_{x} with a center pixel intensity g_{z} , which is the same for all pixels in the neighborhood. Therefore, two crisp sets of pixels can be defined for each pixel neighborhood, as follows:

Let $U = \{0, 1, ..., n-1\}$ be the universal set of all pixels in the $n \times n$ pixel neighborhood. Let $A = \{p_v \in U: \ell_a(x)\}$, where $\ell_A(x)$ is a predicate defined as $g_x \ge g_a$, be the set of all pixels p_x and B be the set of all neighborhood pixels p_{v} with gray value $g_{v} \le g_{c}$ under the universal set U, respectively. Hence, set B is the complement of set A relative to the universal set *U*.

Logically, for crisp set A, the characteristic functions are $\chi(x) = 0$, $p_x \notin A$ and $\chi(x) = 1$, $p_x \in A$. Similarly, the respective characteristic functions for set *B* are $\chi(x) = 0$, $p_x \in B$ and $\chi(x) = 1$, $p_y \notin B$.

Based on these binary values of the characteristic function $\chi(x)$ for a neighborhood of n pixels, a unique LBP code can be calculated as follows:

$$LBP_{code} = \sum_{x=0}^{k-1} d_x \cdot w_x, \tag{1}$$

where $d_{y} = \chi(x)$, $k \in (0, n]$ being the number of pixels in the neighborhood that were considered for the creation of BP and $w_{x} = 2^{x}$, $x \in \{0, 1, ..., k\}$ is a weight function that assigns a weight value at each pixel of the neighborhood. Each pixel of the local neighborhood is characterized by a single LBP code out of 2^k possible codes.

2.2 Fuzzy LBP

A drawback of the LBP method as well as all local descriptors that apply vector quantization is that they are not robust in the sense that a small change in the input image would always cause only a small change in the output. To increase the robustness of the operator, the thresholding function is replaced by two fuzzy membership functions [1]. In order to enhance the LBP approach so that it can handle the uncertainty introduced by the speckle noise, Keramidas et al. [25, 26] incorporated fuzzy logic to the computation of the BPs to cope with inexactness and improve the discrimination power of the LBP approach in noise-degraded images. In this section, we have presented FLBP for texture representation proposed by Iakovidis et al. [21] and Keramidas et al. [27].

The fuzzy logic, as a multi-valued logic, allows intermediate values between the typical values 0/1 or true/false. Fuzzy logic permits the replacement of crisp sets A and B by two fuzzy sets \tilde{A} and \tilde{B} . Members of these fuzzy sets are pixels of the neighborhood that may belong simultaneously to the fuzzy set \tilde{A} (to one degree) and the fuzzy set B (to a different degree). More specifically, pixels with intensity values that are inside the interval $[g_c + T, g_{max}]$ belong to set \tilde{A} , while those with intensity values that are inside the interval $[0, g_c - T]$ belong to set B. Pixels with intensity values that are inside the interval $[g_c - T, g_c + T]$ belong partially to set \tilde{A} and partially to set \tilde{B} . The value of g_{\max} is the maximum intensity value that can be given to a pixel, while T is a parameter that controls the degree of fuzziness of sets \tilde{A} and \tilde{B} . The fuzzy set \tilde{A} under the universal set *U* can be expressed as a set of ordered pairs:

$$\tilde{A} = \{ \langle p_{x}, \mu_{\tilde{a}}(x) \rangle | x \in U \}, \tag{2}$$

where $\mu_A: U \to [0, 1]$ is the degree of the membership to which pixel p_X with gray value g_X is greater than or equal to the gray value of the center pixel g_r , and can be defined as follows:

$$\mu_{\bar{A}}(x) = \begin{cases} 1 & \text{if } g_x \ge g_c + T, \\ 0.5 \left(1 + \frac{(g_x - g_c)}{T} \right) & \text{if } g_c - T < g_x < g_c + T, \ T \ne 0, \\ 0 & \text{if } g_x \le g_c - T, \ T \ne 0, \\ 0 & \text{if } g_x < g_c + T, \ T = 0. \end{cases}$$

$$(3)$$

Similarly, the complement of fuzzy set \tilde{A} can be expressed as

$$\tilde{B} = \{ \langle p_{x}, \mu_{\tilde{R}}(x) \rangle | p_{x} \in U \}, \tag{4}$$

where $\mu_{\tilde{B}}: U \to [0, 1]$ is the degree of membership to which a pixel p_x with gray value g_x is less than the gray value of the center pixel g_x and can be defined as follows:

$$\mu_{\tilde{B}}(x) = 1 - \mu_{\tilde{A}}(x).$$
 (5)

Both $\mu_{\tilde{A}}(x)$ and $\mu_{\tilde{B}}(x)$ for $T \in [0, g_{\max}]$ represent parameter that controls the degree of fuzziness.

It may be noted that for the original LBP operator, a single LBP code characterizes an $n \times n$ pixel neighborhood. However, in the FLBP approach, an $n \times n$ pixel neighborhood can be characterized by more than one LBP code and contribution C_{FLBP} values. The degree to which each LBP code characterizes a neighborhood depends on the membership and non-membership functions $\mu_{\tilde{A}}$ and $\mu_{\tilde{B}}$. When the local neighborhood consists of k sampling points, the resulting histogram has bins numbered $0, 1, ..., 2^k$.

For an $n \times n$ pixel neighborhood, the contribution C_{FLBP} of each LBP code in a single bin i of FLBP histogram is estimated by

$$C_{\text{FLBP}}(x, y, i) = \prod_{r=0}^{k-1} [b_r(i)\mu_{\bar{A}}(x) + (1 - b_r(i))\mu_{\bar{B}}(x)], \tag{6}$$

where $k \in (0, n]$ is the number of neighboring pixels participating in the FLBP code computation, (x, y) denotes the coordinates of a pixel, and $b_r(i) \in \{0, 1\}$ denotes the numerical value of the r^{th} bit of binary representation of bin $i, i = 0, 1, ..., 2^k$. The complete FLBP histogram is computed by summing the contributions of all the pixels in the input image:

$$H_{\text{FLBP}}(i) = \sum_{x, y} C_{\text{FLBP}}(x, y, i), i = 0, 1, ..., 2^{k} - 1,$$
(7)

under the condition

$$\sum_{i=0}^{2^{k}-1} C_{\text{FLBP}}(x, y, i) = 1.$$
 (8)

3 Proposed Method

In order to generalize the FLBP approach so that it can handle the uncertainty with hesitancy originating from imperfect or imprecise information, we propose IFLBP for texture representation using the intuitionistic fuzzy sets as follows.

Let $U = \{0, 1..., n-1\}$ be the universal set for n pixel neighborhood. Then, an intuitionistic fuzzy set \tilde{A} under the universal set U is given by

$$\tilde{A} = \{ \langle p_x, \mu_{\tilde{A}}(x), \nu_{\tilde{A}}(x) \rangle | p_x \in U \}, \tag{9}$$

where $\mu_{\bar{a}}: U \to [0, 1]$ and $\nu_{\bar{a}}: U \to [0, 1]$ denote the degree of membership and non-membership to which an element p_x has either greater or less gray value than g_c in \tilde{A} , respectively, with the condition $0 \le \mu_{\tilde{A}}(x) + \nu_{\tilde{A}}(x) \le 1$. The amount $\pi_{\bar{A}}(x) = 1 - \mu_{\bar{A}}(x) - \nu_{\bar{A}}(x)$, $\forall p_x \in U$ is called the degree of indeterminacy (hesitation part). It is the degree of uncertainty whether p_{ij} belongs to \tilde{A} or not.

The membership and non-membership functions of IFS \tilde{A} can be defined as follows:

$$\mu_{\bar{A}}(x) = \begin{cases} 0 & \text{if } g_{x} < g_{c} - T, \\ 0.5(1+h)\left(1 + \frac{g_{x} - g_{c}}{T}\right) & \text{if } g_{x} \in [g_{c} - T, g_{c}], \ T \neq 0, \\ 0.5\left[\left(1 + \frac{g_{x} - g_{c}}{T}\right) + h\left(\frac{g_{x} - g_{c}}{T}\right) - 1\right)\right] & \text{if } g_{x} \in (g_{c}, g_{c} + T], \ T \neq 0, \\ 1 & \text{if } g_{x} \geq g_{c} + T. \end{cases}$$

$$(10)$$

and

$$\nu_{\bar{A}}(x) = \begin{cases} 1 & \text{if } g_{x} < g_{c} - T, \\ 0.5 \left[\left(1 - \frac{(g_{x} - g_{c})}{T} \right) - h \left(1 + \frac{(g_{x} - g_{c})}{T} \right) \right] & \text{if } g_{x} \in [g_{c} - T, g_{c}], \ T \neq 0, \\ 0.5(1+h) \left(1 - \frac{(g_{x} - g_{c})}{T} \right) & \text{if } g_{x} \in (g_{c}, g_{c} + T], \ T \neq 0, \\ 0 & \text{if } g_{x} \geq g_{c} + T. \end{cases}$$

$$(11)$$

For an $n \times n$ pixel neighborhood, the contribution C_{true} of each IFLBP code in a single bin of IFLBP histogram is estimated as follows:

$$C_{\text{IFLBP}}(x, y, i) = \prod_{r=0}^{k-1} [b_r(i)\mu_{\bar{A}}(x) + (1 - b_r(i))\nu_{\bar{A}}(x)], \tag{12}$$

where $k \in (0, n]$, (x, y) and $b(i) \in \{0, 1\}$ represent the number of neighboring pixels, the coordinates of a pixel and numerical value of the r^{th} bit of binary representation of bin i, respectively. The complete IFLBP histogram is given by

$$H_{\text{IFLBP}}(i) = \sum_{x,y} C_{\text{IFLBP}}(x, y, i), i = 0, 1, ..., 2^{k} - 1.$$
(13)

It may be noted that using the crisp LBP operator, each $n \times n$ pixel neighborhood always contributes to one bin of the histogram; however, in case of both FLBP and IFLBP histograms, each $n \times n$ pixel neighborhood typically contributes to more than one bin of the histogram. The sum of the contribution of an each $n \times n$ pixel neighborhood (IFLBP code) to the bins of the IFLBP histogram is equal to 1, that is

$$\sum_{i=0}^{2^{k}-1} C_{\text{IFLBP}}(x, y, i) = 1.$$
 (14)

An example of IFLBP computation scheme for a 3×3 pixel neighborhood is shown in Figure 1.

Remark 3.1: When $T \neq 0$, h = 0, the resulting intuitionistic fuzzy membership and non-membership functions given by Eqs. (10) and (11) are almost equivalent to the fuzzy membership function $\mu_{\alpha}(x)$ given by Eq. (3), the difference being that $\mu_{\bar{A}}(x) = v_{\bar{A}}(x) = 0.5$ whereas $\mu_{A}(x) = 1$ when $g_{i} = g_{c}$.

Remark 3.2: When T = 0, the resulting intuitionistic fuzzy membership and non-membership functions are equivalent to the crisp thresholding function $\chi_{A}(x)$.

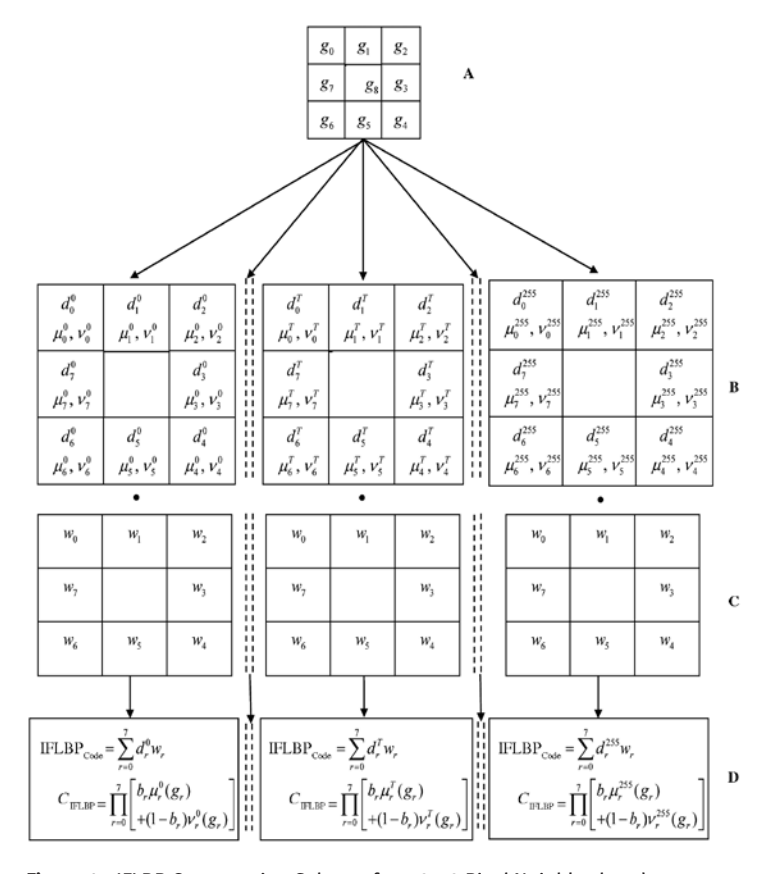


Figure 1: IFLBP Computation Scheme for a 3×3 Pixel Neighborhood. (A) Gray levels of a 3×3 pixel neighborhood. (B) Intuitionistic fuzzy threshold values along with membership and non-membership values. (C) Binomial weights matrix. (D) IFLBP codes and CIFLBP.

4 Performance Metrics: Entropy of IFLBP Features

The information content of an image is often measured by calculating the uncertainty or entropy of an image. As the magnitude of entropy increases, more information is associated with the image. The entropy measures the average, global information content of an image in terms of average bits per pixel.

Shannon entropy [41] is defined as

$$H = -\sum_{i=0}^{255} p_i \log p_i \tag{15}$$

where p_i is the probability of the i^{th} pattern.

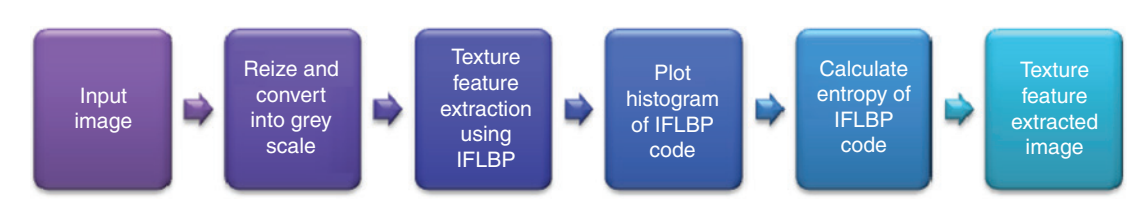


Figure 2: Proposed Model.

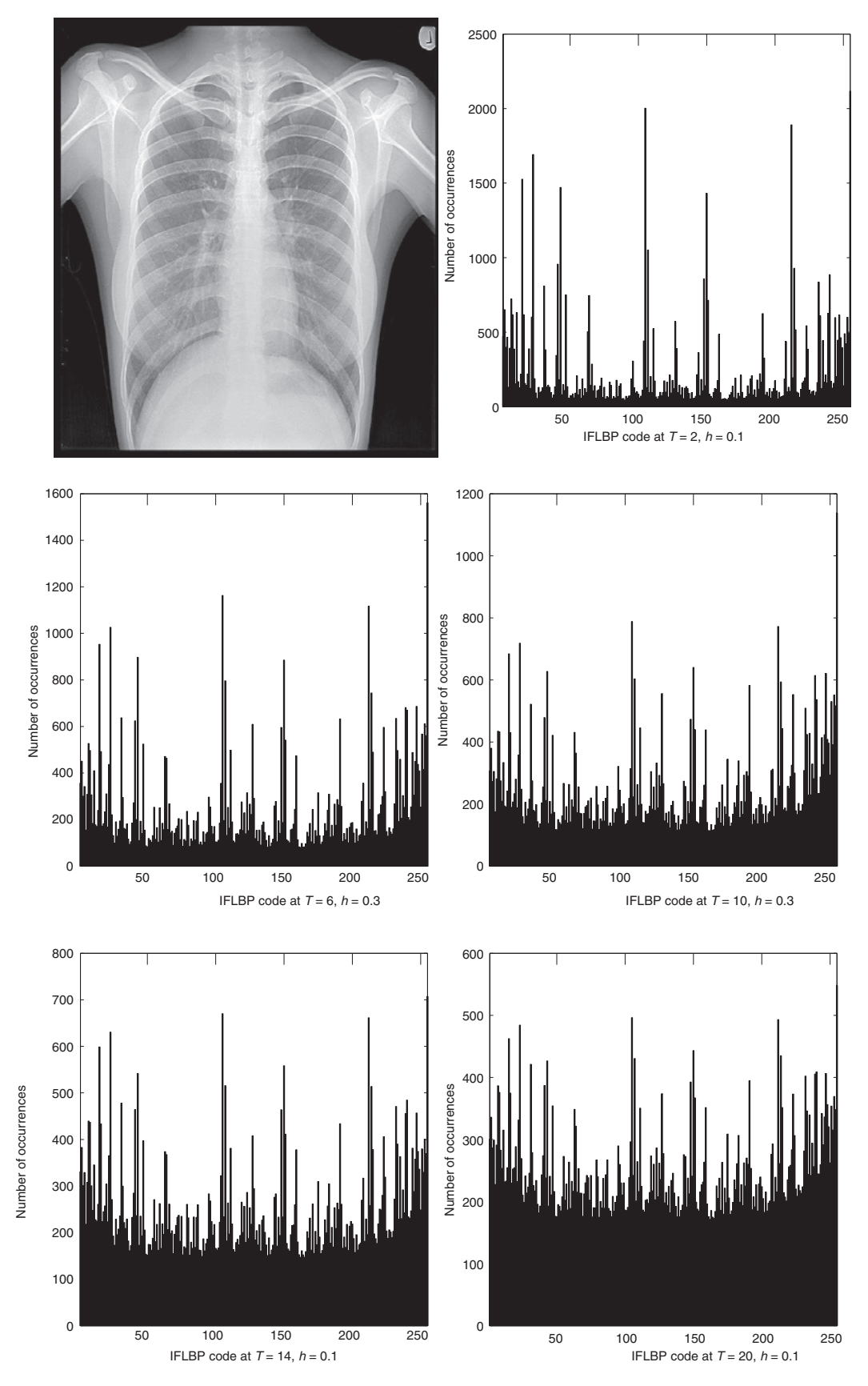


Figure 3: Histogram Plot of IFLBP Codes for X-ray Image.

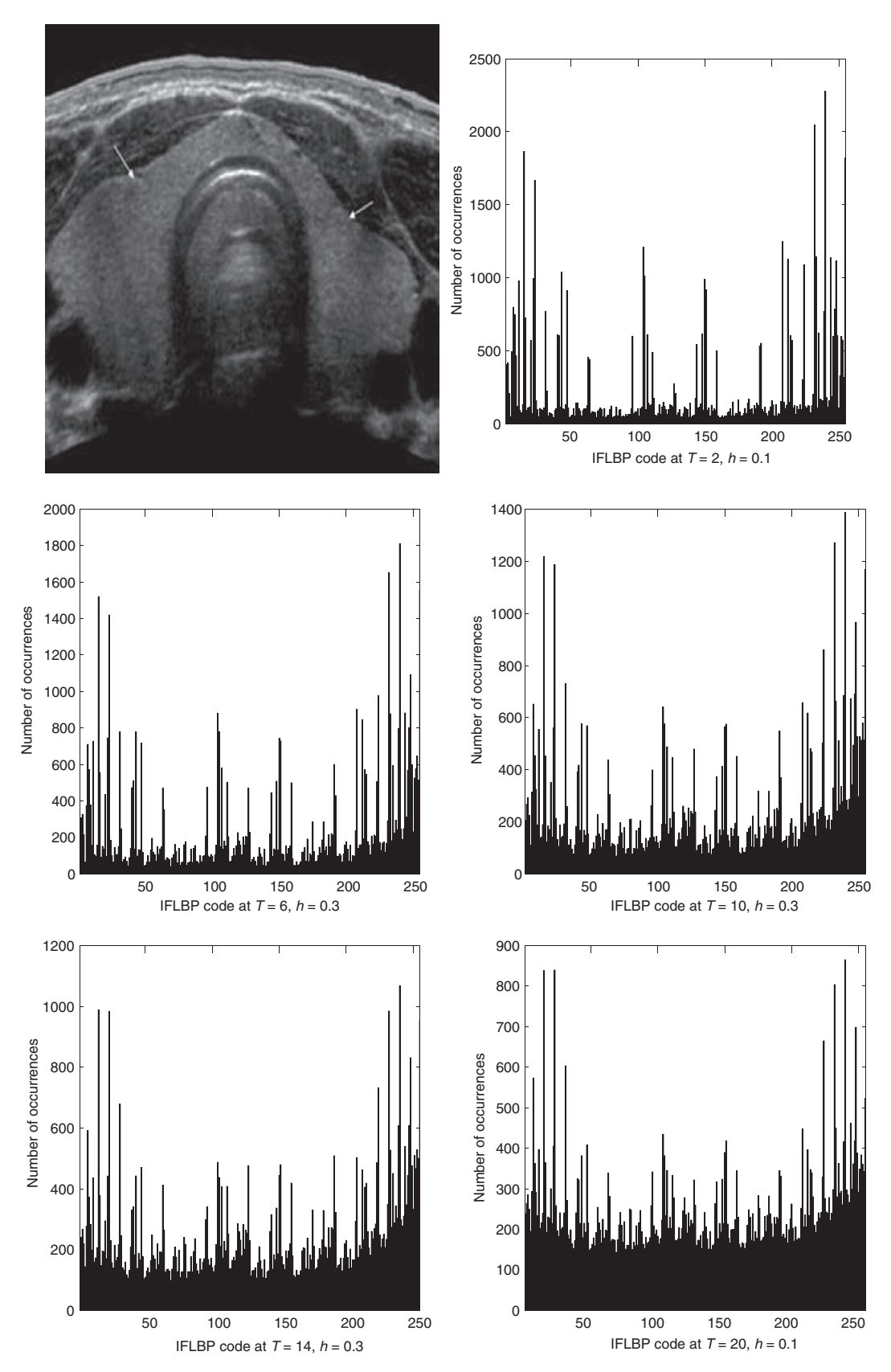


Figure 4: Histogram Plot of IFLBP Codes for Thyroid Image.

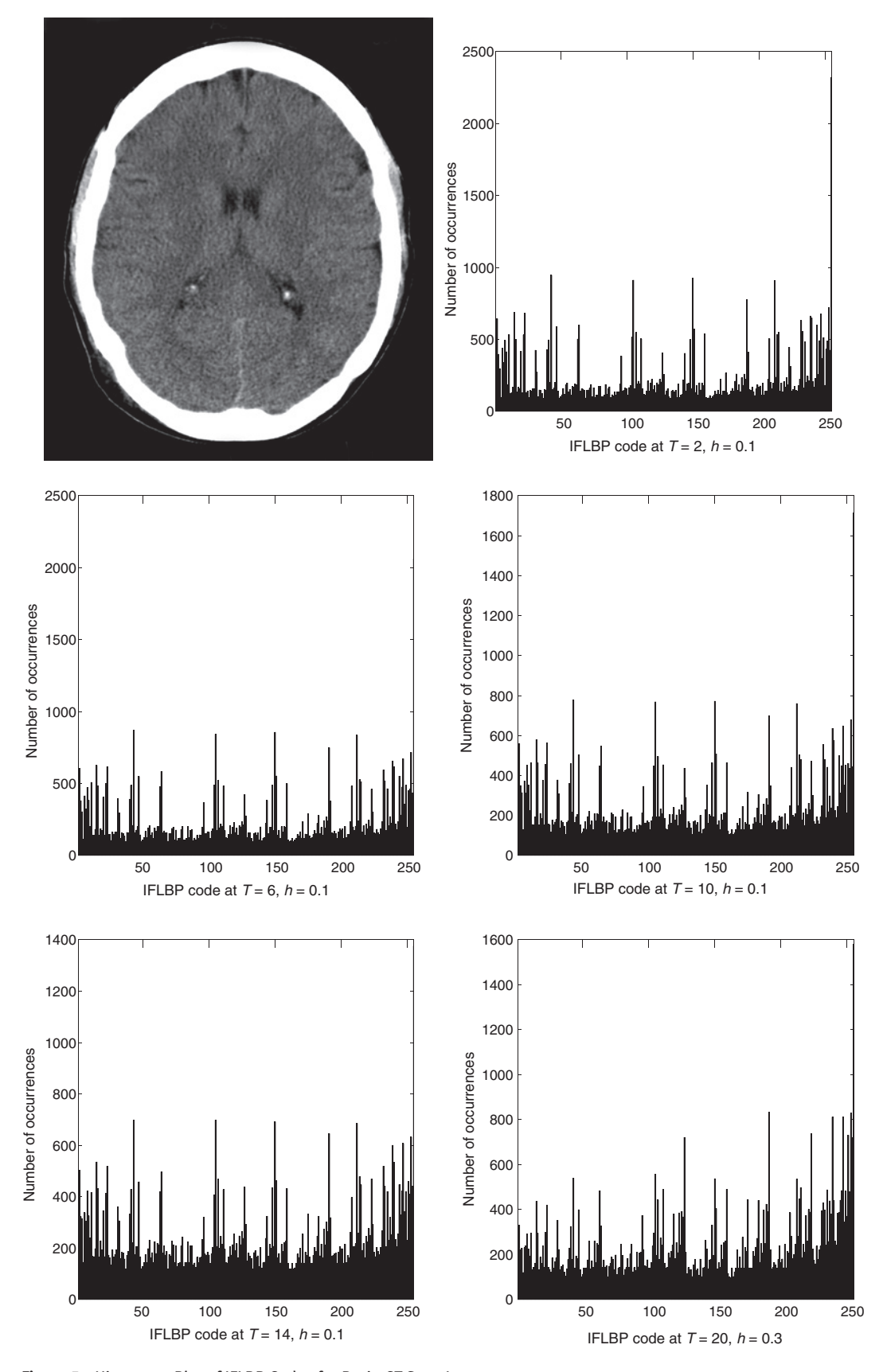


Figure 5: Histogram Plot of IFLBP Codes for Brain CT Scan Image.

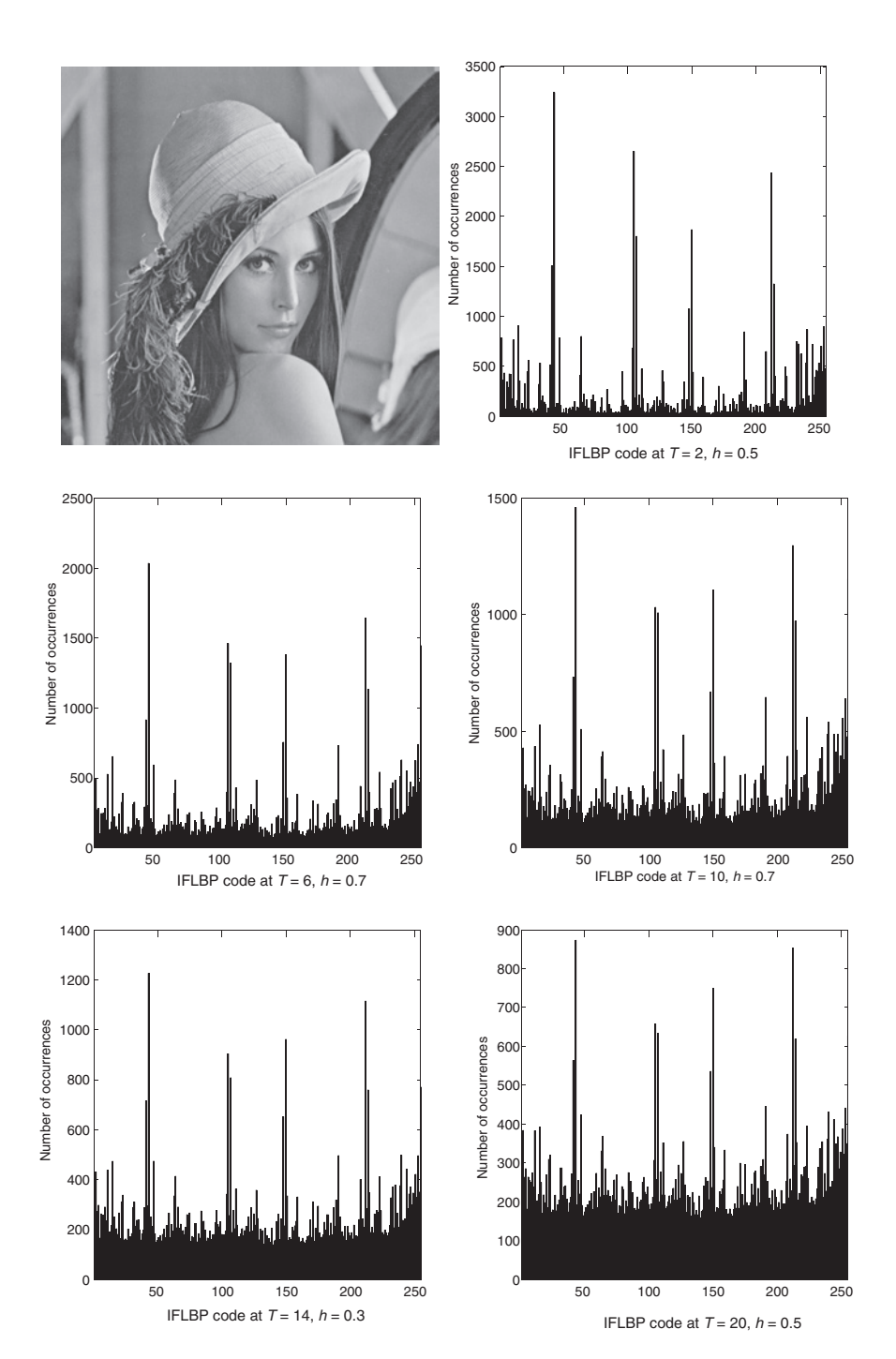


Figure 6: Histogram Plot of IFLBP Codes for Lena Image.

It is worth mentioning that in the logarithmic entropic measure [Eq. (15)], as $p_i \to 0$, its corresponding self-information of this event, $I(p_i) = -\log p_i \to \infty$ but $I(p_i = 1) = \log p_i \to 0$. Thus, we see that information gain from an event is neither bounded at both ends nor defined at all points. In practice, the gain in information from an event, whether highly probable or highly unlikely, is expected to lie between two finite limits. For example, as more and more pixels in an image are analyzed, the gain in information increases, and when all the pixels are inspected, the gain attains its maximum value irrespective of the content of an image.

In Shannon's entropy, which is highly praised, we find that the measure of self-information of an event with probability p_i is taken as $\log p_i$, a decreasing function of p_i . The same decreasing character alternatively

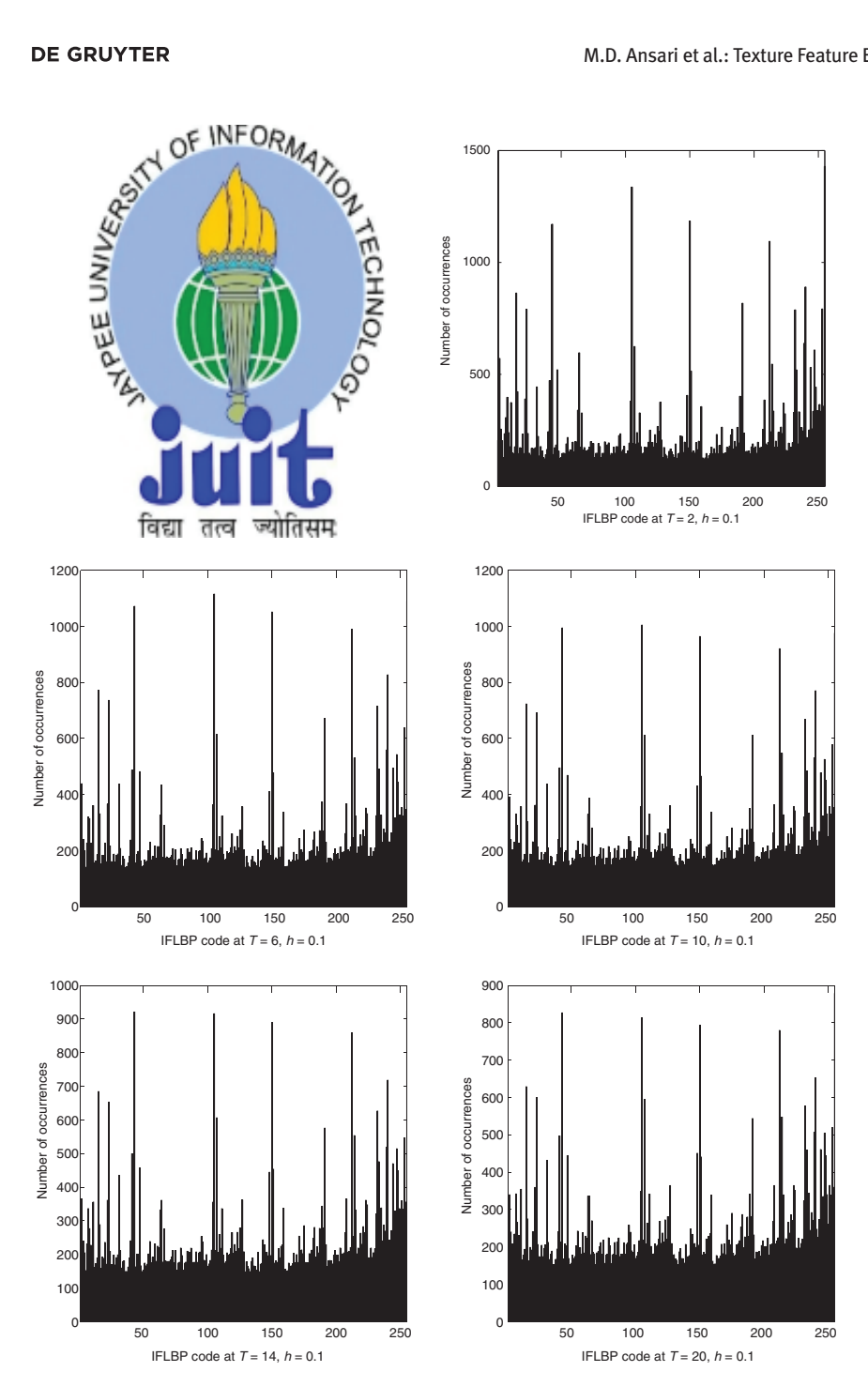


Figure 7: Histogram Plot of IFLBP Codes for JUIT Logo.

may be maintained by considering it as a function of $(1-p_i)$ rather than of $1/p_i$. The additive property, which is considered crucial in Shannon's approach, of the self-information function for independent events may not have a strong relevance (impact) in practice as well as in some situations. Alternatively, as in the case of probability law, the joint self-information may be the product rather than the sum of the self-information in two independent cases. The above considerations suggest the self-information as an exponential function of (1-p) instead of logarithmic behavior. This is also appropriate while considering the concept of information gain in an image. Pal and Pal entropy [35] is defined by

$$H = \sum_{i=0}^{255} p_i e^{1-p_i}.$$
 (16)

Table 1: Entropy Values at Different Thresholds and Hesitation for X-ray Image.

Methods	Hesitation $(h)\downarrow$	Threshold						
		2	6	10	14	20		
Keramidas et al. [27]	0.0	1.9016	1.68193	0.8708	0.5800	0.3889		
Ansari et al. [2]	0.1	1.8530	1.6693	0.8570	0.5997	0.3815		
	0.3	1.7715	1.6195	1.0229	0.5905	0.4978		
	0.5	1.7941	1.6513	1.2770	0.8684	0.5713		
	0.7	1.7825	1.8069	1.7239	1.5165	1.1406		
	1.0	1.6766	1.6686	1.4254	1.3292	1.3247		
Proposed method	0.1	2.6884	2.6999	2.6999	2.7058	2.7068		
	0.3	2.6877	2.7001	2.7040	2.7056	2.7065		
	0.5	2.6844	2.6983	2.7024	2.7040	2.7048		
	0.7	2.6751	2.6923	2.6970	2.6987	2.6995		
	1.0	2.6167	2.6474	2.6538	2.6549	2.6540		

Bold value indicates maximum entropy in a bin.

 Table 2:
 Entropy Values at Different Thresholds and Hesitation for Thyroid Image.

Methods	Hesitation (h)↓	Thresholds (7)—						
		2	6	10	14	20		
Keramidas et al. [27]	0.0	1.6859	1.9053	1.6529	0.8107	0.5882		
Ansari et al. [2]	0.1	1.7407	1.8767	1.6371	1.0325	0.5531		
	0.3	1.8344	1.8491	1.6540	1.1170	0.5800		
	0.5	1.7409	1.8557	1.6227	1.4990	0.6631		
	0.7	1.6966	1.8292	1.7060	1.4552	0.8107		
	1.0	1.3570	1.6481	1.6132	1.3624	0.8700		
Proposed method	0.1	2.6854	2.6938	2.6997	2.7031	2.7055		
	0.3	2.6842	2.6938	2.7000	2.7033	2.7054		
	0.5	2.6800	2.6914	2.6982	2.7016	2.7037		
	0.7	2.6669	2.6822	2.6902	2.6940	2.6961		
	1.0	2.5672	2.5988	2.6106	2.6152	2.6169		

Bold value indicates maximum entropy in a bin.

 Table 3:
 Entropy Values at Different Thresholds and Hesitation for Brain CT Scan Image.

Methods	Hesitation (<i>h</i>)↓	Thresholds (7						
		2	6	10	14	20		
Keramidas et al. [27]	0.0	1.6118	1.4533	0.8742	0.7741	0.5749		
Ansari et al. [2]	0.1	1.6143	1.5051	1.1713	1.0018	0.6372		
	0.3	1.7682	1.7247	1.7263	1.5873	1.2027		
	0.5	1.7776	1.8007	1.7948	1.7139	1.6238		
	0.7	1.4923	1.4875	1.5137	1.5539	1.6139		
	1.0	1.1053	1.1505	1.1139	1.1621	1.1341		
Proposed method	0.1	2.6978	2.6998	2.7020	2.7038	2.7055		
	0.3	2.6933	2.6958	2.6987	2.7009	2.7131		
	0.5	2.6784	2.6822	2.6865	2.6901	2.6935		
	0.7	2.6290	2.6362	2.6441	2.6505	2.6567		
	1.0	2.2237	2.2478	2.6888	2.2903	2.2979		

Bold value indicates maximum entropy in a bin.

Table 4: Entropy Values at Different Thresholds and Hesitation for Lena Image.

Methods	Hesitation $(h)\downarrow$		Thre	Thresholds (7)→		
		2	6	10	14	20
Keramidas et al. [27]	0.0	1.7785	1.6843	1.1374	0.6021	0.4921
Ansari et al. [2]	0.1	1.7785	1.6843	0.9180	0.5782	0.4859
	0.3	1.7718	1.6040	0.7613	0.5782	0.4589
	0.5	1.7921	1.5580	0.9119	0.6599	0.5320
	0.7	1.7935	1.5909	1.2017	0.8528	0.7343
	1.0	1.8024	1.5971	1.4603	1.4030	1.4637
Proposed method	0.1	2.6764	2.6936	2.6998	2.7029	2.7051
	0.3	2.6676	2.6959	2.7016	2.7041	2.7059
	0.5	2.6776	2.6959	2.7016	2.7041	2.7059
	0.7	2.6678	2.6970	2.7017	2.7036	2.7048
	1.0	2.6769	2.6965	2.7000	2.7008	2.7007

Bold value indicates maximum entropy in a bin.

Table 5: Entropy Values at Different Thresholds and Hesitation for JUIT Logo.

Methods	Hesitation (h) \downarrow	Thresholds (T)-					
		2	6	10	16	20	
Keramidas et al. [27]	0.0	0.7454	0.7087	0.6803	0.6768	0.6258	
Ansari et al. [2]	0.1	0.9311	0.6210	0.6033	0.5662	0.5249	
	0.3	1.7927	1.7443	1.7103	1.6453	1.5690	
	0.5	1.8470	1.8102	1.7920	1.7842	1.7757	
	0.7	1.5003	1.5689	1.5803	1.5624	1.6087	
	1.0	1.1239	1.0441	1.0343	1.0431	1.0514	
Proposed method	0.1	2.7010	2.7032	2.7040	2.7046	2.7051	
	0.3	2.6969	2.6996	2.7005	2.7010	2.7016	
	0.5	2.6822	2.6858	2.6867	2.6871	2.6876	
	0.7	2.6302	2.6341	2.6340	2.6337	2.6333	
	1.0	2.1837	2.1643	2.1480	2.1369	2.1266	

Bold value indicates maximum entropy in a bin.

5 Experimental Results and Analysis

It can be observed that the Keramidas et al. method [27] and the Ansari and Ghrera method [2] have zero values for some bins out of 255 bins. However, the proposed method histograms do not have bins with zero values and there are more spikes, though limited in magnitude. This indicates that the Ansari and Ghrera method [2] is more informative than the Keramidas method [27], and the proposed method is more informative than existing methods. Entropy is a measure of uncertainty associated with random occurrences, normally considered as the measure of "disorder". Pal and Pal entropy [35] is a statistical measure of randomness that can be used to characterize the texture of an input image (Figure 2).

The more diversified signal implies higher entropy and more actual information gain. If all the bins of the histogram have equal probability, then the maximum entropy will be reached. Apparently, for the fixed threshold T, the histograms of the proposed method always give greater entropy than the histograms of the existing method. However, the histograms of the Ansari method [2] for the same threshold and using hesitation threshold values $h \in [0, 1]$ give greater entropy than the histograms of the Keramidas method [27]. Therefore, the IFLBP histogram gains more information than the histograms of other reported methods.

Additionally, we apply the proposed IFLBP approach on various images as shown in Figures 3–7 of size 256×256 to calculate the histogram feature vectors for different threshold values and varying hesitation $(h \in [0, 1])$, as well as computed entropies from these histograms; finally, the results are shown in Tables 1–5. We can examine from these tables that the maximum entropies obtained in Table 1 for T=6 and T=10 are at h=0.3, and those for T=2, T=14, T=20, and T=12 are at h=0.1. We follow the same procedure for the remaining images; the results are shown in Tables 2–5 and Figures 4–7. Therefore, the entropies obtained by the proposed method are always greater than the entropies obtained by existing methods. We plot the histograms of IFLBP codes of every image where we have found the maximum entropy, as shown in Figures 3–7. From these histograms, we can observe that the IFLBP histograms do not have bins with zero values. In addition, the IFLBP features of all images are more informative than existing features.

6 Conclusions and Future Work

We have proposed a novel IFLBP for texture feature extraction to encode local texture from an image by incorporating the intuitionistic fuzzy set theory in the representation of local patterns of texture in the images. The proposed method is an extension of the FLBP approach. IFLBP also contributes to more than one bin in the distribution of the IFLBP values. Further, it can be used as a feature vector in various tasks. The proposed IFLBP approach is experimentally evaluated for various medical and image processing images of size 256×256. It can be observed from Tables 1–5 that the entropy values of the proposed method are always greater than those of the existing approaches. The obtained results validate the effectiveness and usefulness of our proposed method over the existing feature extraction methods. The proposed IFLBP approach can be applied for feature extraction in the various fields of image processing and biomedical image processing, i.e. image forgery detection, image segmentation, image de-noising problems, pattern classification and recognition, etc.

Acknowledgments: The authors are sincerely thankful to the editor and anonymous reviewers for their critical comments and suggestions to improve the quality of this work.

Bibliography

- [1] T. Ahonen and M. Pietikäinen, Soft histograms for local binary patterns, in: Proceedings of the Finnish Signal Processing Symposium, FINSIG, vol. 5, p. 1, 2007.
- [2] M. D. Ansari and S. P. Ghrera, Intuitionistic fuzzy local binary pattern for features extraction, Int. J. Inf. Commun. Technol., in press.
- [3] M. D. Ansari, S. P. Ghrera and V. Tyagi, Pixel-based image forgery detection: a review, IETE J. Educ. 55.1 (2014), 40–46.
- [4] M. D. Ansari, S. P. Ghrera and M. Wajid, An approach for identification of copy-move image forgery based on projection profiling, Pertan. J. Sci. Technol., in press.
- [5] K. T. Atanassov, Intuitionistic fuzzy sets, Fuzzy Sets Syst. 20 (1986), 87-96.
- [6] K. T. Atanassov and G. Gargov, Interval-valued intuitionistic fuzzy sets, Fuzzy Sets Syst. 31 (1989), 343-349.
- [7] A. Barcelo, E. Montseny and P. Sobrevilla, Fuzzy texture unit and fuzzy texture spectrum for texture characterization, Fuzzy Sets Syst. 158 (2007), 239-252.
- [8] G. Castellano, L. Bonilha, L. M. Li and F. Cendes, Texture analysis of medical images, Clin. Radiol. 59 (2004),
- [9] C. Chan, J. Kittler and K. Messer, Multi-scale local binary pattern histograms for face recognition, in: ICB 2007, Seoul, Korea, LNCS 4642, pp. 809-818, Springer, 2007.
- [10] T. W. S. Chow and M. K. M. Rahman, A new image classification technique using tree-structured regional features, Neurocomputing 70 (2007), 1040-1050.
- [11] A. Destrero, C. De Mol, F. Odone and A. Verri, A regularized framework for feature selection in face detection and authentication, Int. J Comput. Vis. 83 (2009), 164-177.
- [12] J. Fehr, Rotational invariant uniform local binary patterns for full 3D volume texture analysis, in: FINSIG 2007, Oulu, Finland, 2007.
- [13] R. Garcia, X. Cufi and J. Batlle, Detection of matchings in a sequence of underwater images through texture analysis, in: Proc. IEEE International Conference on Image Processing, vol. 1, pp. 361–364, 2001.

- [14] H. Grabner, T. T. Nguyen, B. Gruber and H. Bischof, On-line boosting-based car detection from aerial images, ISPRS J. Photogramm. Remote Sens. 63 (2008), 382-396.
- [15] D. Grangier and S. Bengio, A discriminative kernel-based approach to rank images from text queries, IEEE Trans. Pattern Anal. Mach. Intell. 30 (2008), 1371-1384.
- [16] H. Hadizadeh and S. Baradaran Shokouhi, Random texture defect detection using 1-D hidden Markov models based on local binary patterns, IEICE Trans. Inform. Syst. 91 (2008), 1937-1945.
- [17] A. Hafiane, G. Seetharaman and B. Zavidovique, Median binary pattern for textures classification, ICIAR 4633 (2007), 387-398.
- [18] A. Hafiane, G. Seetharaman, K. Palaniappan and B. Zavidovique, Rotationally invariant hashing of median binary patterns for texture classification, Proc. Image Anal. Recognit. LNCS (2008), 619-629.
- [19] M. Heikkila and M. Pietikainen, A texture-based method for modeling the background and detecting moving objects, IEEE Trans. Pattern Anal. Mach. Intell. 28 (2006), 657-662.
- [20] D. K. lakovidis, D. Maroulis and S. Karkanis, An intelligent system for automatic detection of gastrointestinal adenomas in video endoscopy, Comput. Biol. Med. 36 (2006), 1084-1103.
- [21] D. K. lakovidis, E. G. Keramidas and D. Maroulis, Fuzzy local binary patterns for ultrasound texture characterization, in: Image Analysis and Recognition, pp. 750-759, Springer, Berlin, 2008.
- [22] J. livarinen, Surface defect detection with histogram-based texture features, in: Intelligent Robots and Computer Vision XIX: Algorithms, Techniques, and Active Vision, vol. 4197, pp. 140–145, 2000.
- [23] J. Jiang, A. Armstrong and G. C. Feng, Web-based image indexing and retrieval in JPEG compressed domain, Multimed. Syst. 9 (2004), 424-432.
- [24] E. G. Keramidas, Ultrasound image processing and analysis framework, MSc thesis, University of Athens, Greece, 2007.
- [25] E. G. Keramidas, D. K. lakovidis and D. Maroulis, Noise-robust statistical feature distributions for texture analysis, in: Signal Processing Conference, 2008 16th European, pp. 1–5, IEEE, 2008.
- [26] E. G. Keramidas, D. K. Iakovidis, D. Maroulis and N. Dimitropoulos, Thyroid texture representation via noise resistant image features, IEEE Int. Symp. Comput. Based Med. Syst. (2008), 560-565.
- [27] E. G. Keramidas, D. K. lakovidis and D. Maroulis, Fuzzy binary patterns for uncertainty-aware texture representation, Electron. Lett. Comput. Vis. Image Anal. 10 (2011), 63-78.
- [28] Y. Li and J. X. Peng, Remote sensing texture analysis using multi-parameter and multi-scale features, Photogramm. Eng. Remote Sens. 69 (2003), 351-356.
- [29] C. J. Liao and S. Y. Chen, Complementary retrieval for distorted images, Pattern Recognit. 35 (2002), 1705–1722.
- [30] L. Ma and R. C. Staunton, Optimum Gabor filter design and local binary patterns for texture segmentation, Pattern Recognit. Lett. 29 (2008), 664-672.
- [31] A. R. Mishra, D. Jain and D. S. Hooda, On logarithmic fuzzy measures of information and discrimination, J. Inform. Optim. Sci. 37 (2016), 213-231.
- [32] A. R. Mishra, Intuitionistic fuzzy information with application in rating of township development, Iran. J. Fuzzy Syst. 13 (2016), 49-70,
- [33] L. Nanni and A. Lumini, A reliable method for cell phenotype image classification, Artif. Intell. Med. 43 (2008), 87–97.
- [34] T. Ojala, M. Pietikinen and D. Harwood, A comparative study of texture measures with classification based on featured distribution, Pattern Recognit. 29 (1996), 51-59.
- [35] N. R. Pal and S. K. Pal, Object-background segmentation using new definitions of entropy, IEE Proc. E Comput. Digit. Techn. **136** (1989), 284-295.
- [36] M. Petrou and P. G. Sevilla, Image Processing: Dealing with Texture, Wiley, New York, 2006.
- [37] N. Petrović, L. Jovanov, A. Pižurica and W. Philips, Object tracking using naive Bayesian classifiers, in: International Conference on Advanced Concepts for Intelligent Vision Systems, pp. 775–784, Springer, Berlin Heidelberg, 2008.
- [38] G. Pok, K. H. Ryu and J. Lyu, Rotation and gray-scale invariant classification of textures improved by spatial distribution of features, in: International Conference on Database and Expert Systems Applications, pp. 250-259, Springer, Berlin Heidelberg, 2005.
- [39] O. Sertel, J. Kong, H. Shimada, U. V. Catalyurek, J. H. Saltz and M. N. Gurcan, Computer-aided prognosis of neuroblastoma on whole-slide images: classification of stromal development, Pattern Recognit. 42 (2009), 1093-1103.
- [40] C. Shan, S. Gong and P. W. McOwan, Facial expression recognition based on local binary patterns: a comprehensive study, Image Vis. Comput. 27 (2009), 803-816.
- [41] C. E. Shannon, A mathematical theory of communication, Bell Syst. Techn. J. 27 (1948), 623-656.
- [42] O. Silven, M. Niskanen and H. Kauppinen, Wood inspection with non-supervised clustering, Mach. Vision Appl. 13 (2003), 275-285.
- [43] Z. Stan, C. RuFeng, L. ShengCai and Z. Lun, Illumination invariant face recognition using near-infrared images, IEEE Trans. Pattern Anal. Mach. Intell. 29 (2007), 627-639.
- [44] F. Tajeripour, E. Kabir and A. Sheikhi, Fabric defect detection using modified local binary patterns, EURASIP J. Adv. Signal Process. 2008 (2008), 783-898.
- [45] D. P. Tian, A review on image feature extraction and representation techniques, Int. J. Multimed. Ubiq. Eng. 8.4 (2013), 385–396.
- [46] O. Tsymbal, V. Lukin, N. Ponomarenko, A. Zelensky, K. Egiazarian and J. Astola, Three-state locally adaptive texture preserving filter for radar and optical image processing, EURASIP J. Adv. Signal Process. 8 (2005) 1185-1204.

- [47] T. Wagner, Texture analysis, in: Handbook of Computer Vision and Application, Academic Press, Orlando, FL, 1999.
- [48] Z. Wang and J. H. Yong, Texture analysis and classification with linear regression model based on wavelet transform, IEEE Trans. Image Process. 17 (2008), 1421–1430.
- [49] W. Wu, J. Li, T. Wang and Y. Zhang, Markov chain local binary pattern and its application to video concept detection, in: 15th *IEEE International Conference on Image Processing*, pp. 2524–2527, IEEE, 2008.
- [50] C. H. Yao and S. Y. Chen, Retrieval of translated, rotated and scaled color textures, Pattern Recognit. 36 (2003), 913-929.
- [51] L. Zadeh, Fuzzy sets, J. Inform. Control 8 (1965), 338-353.
- [52] X. Zhang, Y. Gao and M. Leung, Recognizing rotated faces from frontal and side views: an approach toward effective use of mugshot databases, IEEE Trans. Inform. Forens. Secur. 3 (2008), 684-697.